

**Primary oxide minerals in the system  $\text{WO}_3 - \text{Nb}_2\text{O}_5 - \text{TiO}_2 - \text{Fe}_2\text{O}_3 - \text{FeO}$  and their breakdown products from the pegmatite No. 3 at Dolní Bory - Hatě, Czech Republic**

Milan Novák<sup>1\*</sup>, Zdeněk Johan<sup>2</sup>, Radek Škoda<sup>1</sup>, Petr Černý<sup>3</sup>, Vladimír Šrein<sup>4</sup> and František Veselovský<sup>5</sup>

<sup>1</sup> *Department of Geological Sciences, Masaryk University, Kotlářská 2, 611 37 Brno, Czech Republic*

<sup>2</sup> *BRGM, 3, avenue Claude Guillemin B.P. 6009, F-45060 Orléans, Cedex 2, France*

<sup>3</sup> *Department of Geological Sciences, University of Manitoba, Winnipeg, R3T 2N2 Manitoba, Canada*

<sup>4</sup> *Institute of Rock Mechanics, Academy of Sciences of Czech Republic, V Holešovičkách 41, 182 09 Praha, Czech Republic*

<sup>5</sup> *Czech Geological Survey, Klárov 3, 118 21 Praha, Czech Republic.*

## Abstract:

Symmetrically zoned barren pegmatite dike No. 3 cuts granulite at Dolní Bory - Hatě, Czech Republic. It contains minor to accessory biotite, schorl, muscovite, sekaninaite, andalusite, diaspore, apatite and several rare accessory minerals. Black, tabular crystals of ferberite-*wolframoixiolite* occur almost exclusively in an andalusite-diaspore aggregate with sequential accumulations of late pyrophyllite, kaolinite and muscovite-illite. Complex zoning of the individual crystals of ferberite-*wolframoixiolite* shows primary, coarse oscillatory zoning consisting of narrow zones of ferberite (5.01-6.00 apfu W) and dominant niobian ferberite I (5.00-3.01 apfu W) to *wolframoixiolite* (< 3.00 apfu W), the latter two phases with very fine oscillatory internal zoning. The primary phases were locally replaced by a fine-grained mixture of ferberite to niobian ferberite II > tungstenian-titanian ferrocolumbite >> niobian and tungstenian rutile > ScPO<sub>4</sub> phase > scheelite. Primary and secondary phases are characterized by large variation in W/(W+Nb+Ta) and calculated Fe<sup>2+</sup>/(Fe<sup>2+</sup>+Fe<sup>3+</sup>) but low and almost constant Mn/(Mn+Fe<sub>tot</sub>) and Ta/(Ta+Nb). The contents of P, U, Ti, Zr, Si, Sc, Al and Ca vary from negligible in ferberite to minor in *wolframoxiolite* and its U-rich variety: UO<sub>2</sub> 2.71 (19.82 U-rich variety), P<sub>2</sub>O<sub>5</sub> 0.30, TiO<sub>2</sub> 4.81, ZrO<sub>2</sub> 2.84, SiO<sub>2</sub> 0.93, Sc<sub>2</sub>O<sub>3</sub> 4.36, Al<sub>2</sub>O<sub>3</sub> 0.87, CaO 1.02 (all in wt.%). The combined exchange vector: (R<sup>3+</sup>)<sub>8</sub>(R<sup>4+</sup>)<sub>6</sub>(R<sup>5+</sup>)<sub>16</sub>(R<sup>2+</sup>)<sub>13</sub>(R<sup>6+</sup>)<sub>17</sub>, where R<sup>2+</sup> = Fe<sup>2+</sup> > Mn, Ca; R<sup>3+</sup> = Fe<sup>3+</sup> > Sc, Al; R<sup>4+</sup> = Ti > Zr, Si, U; R<sup>5+</sup> = Nb > Ta, P; R<sup>6+</sup> = W, seems to be the best expression of the actual substitution mechanism from ferberite to *wolframoxiolite* with the theoretical end composition (R<sup>2+</sup><sub>1.1</sub>R<sup>3+</sup><sub>3.4</sub>R<sup>4+</sup><sub>1.9</sub>R<sup>5+</sup><sub>5.6</sub>)<sub>Σ12</sub>O<sub>24</sub>. The homovalent substitutions expressed by the exchange vectors: Fe<sup>2+</sup>Mn<sub>-1</sub>, TaNb<sub>-1</sub> and ScFe<sup>3+</sup><sub>-1</sub> are rather negligible. Formation of primary W,Nb,Fe-oxide minerals is closely related to the assemblage andalusite+diaspore, formed at T < ~400 °C for P = 2 kbar. The breakdown process probably proceeded at slightly lower temperatures at about 350-300 °C. Textural relations of the breakdown products characterized by the total absence of any depleted primary phase in the BSE images indicate that the secondary assemblage did not originate by an exsolution-type process. Complete recrystallization and reconstitution of the primary minerals seems to be responsible for its origin. The chemical composition of the primary niobian ferberite to *wolframoixiolite* from Dolní Bory - Hatě is distinct from all other W-rich Nb,Ta-oxide minerals described to date except niobian wolframite from the granitic pegmatite at Nuaparra, Mozambique.

Key words: tungsten, ferberite, *wolframoixiolite*, columbite, rutile, electron microprobe, miscibility, subsolidus breakdown, granitic pegmatite, Dolní Bory - Hatě, Czech Republic

## 1. Introduction

Niobium-tantalum oxide minerals with substantial amounts of W have been sporadically reported from granitic pegmatites (Černý & Ercit, 1985, 1989 and references therein), and exceptionally from hydrothermal wolframite-quartz veins (Amichba & Dubakina, 1974; Beddoe-Stephens & Fortey, 1981; Tindle & Webb, 1989). Several new occurrences of commonly microscopic grains of W-rich Nb,Ta-oxide minerals were described in the last decade from rare-element pegmatites, granites and rhyolites (Johan & Johan, 1994; Raimbault & Burnol, 1998; Tindle *et al.* 1998; Novák & Černý, 1998a; Aurisicchio *et al.*, 2002; Černý *et al.*, 2007; Breiter *et al.* 2007). On the basis of their chemical composition, they were termed niobian wolframite, tungstenian columbite, tungstenian ixiolite, *wolframoixiolite* or *W-ixiolite*, and *wolframowodginite*; however, in many cases their structural type was not determined because of the microscopic size of crystals did not permit X-ray diffraction.

Tungsten-rich Nb,Ta-oxide minerals are known from distinct types and subtypes of granitic pegmatites (Černý & Ercit, 2005) ranging from geochemically primitive pegmatites with simple mineral assemblages including common minerals such as biotite, muscovite, tourmaline, andalusite, apatite and sekaninaite (Novák & Šrein, 1989) to highly evolved, Li-rich, complex pegmatites of elbaite and petalite subtypes (Konovalenko *et al.*, 1982; Tindle *et al.*, 1998; Aurisicchio *et al.*, 2002). Based on the published data, most examined pegmatites containing W-rich Nb,Ta-oxide minerals belong to the LCT family; however, elevated W contents were also found in Nb,Ta,Ti-oxide minerals from typical NYF pegmatites (Aurisicchio *et al.*, 2001; Škoda *et al.*, 2006).

The pegmatite dike No. 3 from Dolní Bory-Hatě, western Moravia, Czech Republic belongs to the rather primitive pegmatites. Novák & Šrein (1989) and Novák & Černý (1998a) published electron-microprobe data for ferberite and associated minerals, some of them with high contents of Sc. Here we describe paragenetic relations of primary W,Nb,Fe-oxide minerals - ferberite to *wolframoixiolite*, and their secondary breakdown products – ferberite to niobian ferberite, tungstenian-titanian ferrocolumbite, niobian and tungstenian rutile, a ScPO<sub>4</sub> phase and scheelite. This unique assemblage is restricted to the system WO<sub>3</sub> – Nb<sub>2</sub>O<sub>5</sub> – TiO<sub>2</sub> – Fe<sub>2</sub>O<sub>3</sub> – FeO (with limited local participation of Sc, Zr and P), which has no analog in the extant literature, and which permits examination of coexisting primary phases and their alteration products. We discuss textural relations and chemical composition of the W,Nb,Fe-oxide phases, their substitution mechanisms, and miscibility of these minerals at given P-T-X conditions of their formation.

## 2. Geological setting and occurrence

The examined pegmatite dike is located in the Hatě area, W of the Dolní Bory village, in the Bory pegmatite district (Fig. 1), western Moravia, Czech Republic (Novák *et al.*, 1992). This pegmatite district is located within the area of granulitic rocks of the Bory granulite massif surrounded by cordierite migmatites and biotite-sillimanite migmatitic gneisses of the Moldanubian Zone. The district comprises three types of granitic pegmatites with distinctly different degrees of fractionation: (i) Less evolved, symmetrically zoned barren pegmatite dikes with schorl, muscovite, apatite and locally also with andalusite and sekaninaite are the most abundant (Staněk, 1954, 1997). (ii) More evolved, phosphate-bearing pegmatites characterized by the presence of primary Fe,Mn-phosphates (zwieselite, triplite, triphylite, graftonite, beusite) are less common. They were described from Dolní Bory (dike Oldřich

located in the Hatě area), Cyrilov, Vídeň, Horní Bory, and Rousměrov (Staněk, 1954, 1968, 1997; Škoda *et al.*, 2007). Their mineral assemblages and internal structure indicate close relations to the beryl-columbite-phosphate subtype (Černý & Ercit, 2005); however, beryl is absent in the whole pegmatite district. (iii) The most evolved lepidolite-subtype pegmatites with abundant elbaite, locally amblygonite-montebrazite, cookeite and spodumene+quartz pseudomorphs after petalite are rare, located at Dobrá Voda, Dolní Bory (dike No. 21 in the Hatě area), and Laštovičky (Staněk 1973; Němec 1981; Novák & Staněk, 1999). All these pegmatites, whose geochemical characteristics indicate the LCT affiliation, belong to a single pegmatite population likely derived from related parental granites. The U-Pb radiometric data on monazite from the phosphate-bearing pegmatite dike Oldřich, Dolní Bory-Hatě showed  $335.8 \pm 2$  and  $337.2 \pm 2$  Ma (Novák *et al.*, 1998) and indicate their Variscan age.

[Fig. 1]

Zoned pegmatites in the Hatě area (including the dike No. 3) are predominantly NNW striking and steeply dipping. They exhibit discordant and sharp contacts with host granulitic rocks. The pegmatite dike No. 3 is about 5 m thick and several tens of meters long. Its internal structure comprises, from contact inwards: granitic border zone of a fine- to medium-grained microcline + quartz + oligoclase + biotite  $\pm$  muscovite; subordinate graphic wall zone of microcline + quartz  $\pm$  muscovite; and a core built up of blocky microcline and massive quartz containing a large andalusite-diaspore nodule (Fig. 2). Minor intermediate albite unit is commonly located between the graphic zone (or blocky microcline) and blocky quartz. This unit contains schorl, muscovite, andalusite, sekaninaite, biotite and apatite in minor to accessory amounts. More details about geology and petrology of pegmatites from the Bory pegmatite district were reported by Staněk (1954, 1997) and Duda (1986).

[Fig. 2]

### 3. Analytical methods

The chemical composition was studied by electron-microprobe analysis on two instruments. (i) CAMECA SX 100 at the Joint Laboratory of Electron Microscopy and Microanalysis, Institute of Geological Sciences, Masaryk University, Brno and Czech Geological Survey, R. Škoda analyst. Element abundances of W, Nb, Ta, P, Ti, Zr, Hf, U, Th, Si, Y, Sc, Sb, Bi, As, Al, Pb, Mn, Mg, Fe, Ca and F were measured in wavelength dispersive mode. The following standards and X-ray lines were used:  $K_{\alpha}$  lines: Ca - andradite, Fe - columbite, Mg, Al - spinel, Mn - rhodonite, P -  $\text{Ca}_5(\text{PO}_4)_3\text{F}$ , Ti - TiO, Sc -  $\text{ScVO}_4$ ;  $L_{\alpha}$  lines: Zr - zircon, Nb - columbite, Hf - metallic Hf, Sn -  $\text{SnO}_2$ , W - metallic W;  $M_{\alpha}$  lines: Pb - PbSe, Ta -  $\text{CrTa}_2\text{O}_6$ , and  $M_{\beta}$  lines: U - metallic U. The accelerating voltage and beam currents were 15 kV and 20 nA, respectively, with beam diameter 1  $\mu\text{m}$ . The raw data were reduced using appropriate PAP matrix corrections (Pouchou & Pichoir, 1985). Major elements were measured for 20 s at the peak and for 10 s for each background. The counting times for minor to trace elements were 40 s and 60 s, respectively, and half time on each background. When only one background and a calculated background slope were applied, the background counting time corresponded to the peak counting time. (ii) CAMECA SX-50 at the BRGM-CNRS electron-microprobe laboratory, Orléans, C. Gilles analyst. Accelerating voltage 20 kV, beam current 20 nA; the following standards and analytical lines were used:  $K_{\alpha}$  lines: Mn, Ti -  $\text{MnTiO}_3$ , Fe -  $\text{Fe}_2\text{O}_3$ , Sc - metal Sc, Si - albite, P - apatite;  $L_{\alpha}$  lines: Zr -  $\text{ZrSiO}_4$ , Nb -  $\text{LiNbO}_3$ ;  $M_{\alpha}$  lines: W - metal W, Ta - microlite. The analytical data were corrected using the PAP correction procedure (Pouchou & Pichoir, 1984, 1985). The normalization on 12 cations and 24 anions per formula unit, assuming valence-charge balance (Ercit *et al.*, 1992), was used

for the calculation of  $\text{Fe}^{3+}$  in all studied minerals and to facilitate mutual comparison of atomic contents (ferberite, *wolframoixiolite*, columbite, rutile).

The qualitative X-ray diffraction work was done with powder Phillips X'pert System (CuK $_{\alpha 1}$  radiation, 40kV/40mA, step 0.02° 2 $\theta$ , time 10 s, graphite secondary monochromater). Samples were placed on silicon wafers from alcohol suspension. Data obtained were processed with the use of the X-ray diffraction software, ZDS-System, version 6.01 (Ondruš & Skála, 1997). Unit cell-parameters were calculated using the Burnham (1962) program with a calibration procedure for eccentricity of the sample.

## 4. Results

### *The andalusite-diaspore nodule-hosted W,Nb,Fe-oxide minerals*

The andalusite-diaspore nodule, about 1 m<sup>3</sup> in diameter, occurred in massive blocky quartz of the quartz core (Fig. 2). It was mined out during the early nineteen fifties, and the samples examined were obtained from the collection of the Moravian Museum, Brno. The andalusite-diaspore aggregate consists of predominant, euhedral to subhedral, columnar to conic crystals of brownish red to pink andalusite, up to 5 cm long, growing outward from the nodule into quartz. Andalusite is locally zoned with pink cores in thin sections. Less abundant thin tabular crystals (lamellae) of grey diaspore, about 1 mm thick and up to 2 cm across, occur exclusively in andalusite from the central part of the nodule. They do not show any regular crystallographic orientation with respect to the zoned andalusite crystals and contain very rare inclusions of foitite. Textural relations of andalusite and diaspore observed in thin sections and BSE images show no replacement features between these minerals. Broken lamellae of diaspore enclosed in massive undeformed andalusite (Fig. 3a,b) suggest that diaspore crystallized earlier. Local sequential accumulations and vein-like aggregates of pyrophyllite, kaolinite and muscovite-illite are common (Fig. 3b). All these late minerals replaced andalusite but left diaspore almost intact (Fig. 3b). Monazite-(Ce), xenotime-(Y) and zircon were found in small grains (~ 1 mm), locally associated with ilmenite and rutile. Additional primary minerals found in the andalusite-diaspore nodule include schorl, foitite, muscovite, augelite and pyrite. Rare secondary autunite-metaautunite occurs in fissures of andalusite and on cleavage planes of diaspore and pyrophyllite, commonly located close to grains of REE-phosphates and zircon. Novák & Taylor (2005) suggested  $T < 400$  °C for  $P_{\text{fluid}} = 2$  kbar for the formation of the assemblage andalusite+diaspore.

[Fig. 3]

### *Complex W,Nb,Fe-oxide minerals*

Black, tabular, subhedral to euhedral crystals of ferberite-*wolframoixiolite*, up to 2 cm in size, occur almost exclusively in the andalusite-diaspore aggregate. Some grains were also found in the assemblage andalusite+quartz close to the nodule margin. Complex zoning of the individual crystals is characteristic: primary, coarse oscillatory zoning consists of narrow zones of ferberite and dominant niobian ferberite I to *wolframoixiolite* (Fig. 4a). The latter two minerals commonly exhibit very fine oscillatory (but locally patchy) internal zones (Fig. 4a,b,c,d). Very rare elongated tiny blebs of U-rich *wolframoixiolite* also are present in the *wolframoixiolite* matrix.

Ferberite, homogeneous in the BSE image (Fig. 4a,d), was not affected by breakdown processes. However, oscillatory zoned niobian ferberite I to *wolframoxiolite* was locally

replaced by aggregates of secondary phases (Fig. 4b,c,d): a fine-grained mixture of subhedral to locally euhedral grains of ferberite to niobian ferberite II (up to 40  $\mu\text{m}$ ) > anhedral grains tungstenian-titanian ferrocolumbite (up to 30  $\mu\text{m}$ ) >> anhedral niobian and tungstenian rutile (up to 20  $\mu\text{m}$ ) > ScPO<sub>4</sub> phase > scheelite. Rutile and the ScPO<sub>4</sub> phase are always closely associated, and they have never been found outside of the secondary aggregate. Their secondary origin, linked to that of the associated ferberite to niobian ferberite II and tungstenian-titanian ferrocolumbite, is obvious, although the source of Zr and P is not necessarily restricted to the primary oxide minerals. The aggregates of secondary phases are randomly distributed within *wolframoixiolite* and less commonly in niobian ferberite I portions (Fig. 4d) of the complexly zoned ferberite-*wolframoixiolite* crystals, with no apparent spatial predisposition of the individual aggregates (Fig. 4a) such as the veining observed in e.g., niobian rutile (see Černý *et al.*, 2000a, 2007).

[Fig. 4]

#### *X-ray powder diffraction*

Powder XRD examination of various parts of zoned ferberite-*wolframoixiolite* crystals, including breakdown products, yielded the unit-cell dimensions close to those of the synthetic ferberite (Table 1). The low-angle peaks with very low intensities indicate the presence of an orthorhombic columbite-type phase. However, diffractions, which would unambiguously identify an ordered columbite structure, were not observed. In view of the high contents of W and Ti, a disordered structure is presumed more probable for this phase. Nevertheless, it is named (tungstenian-titanian) ferrocolumbite and not W,Ti-rich ixiolite in the following text to avoid possible confusion with primary *wolframoixiolite*.

[Table 1]

#### *Chemical composition*

The chemical composition of the primary W,Nb,Fe-oxide minerals, varying from Nb-poor ferberite to compositionally complex *wolframoixiolite*, show a complete miscibility. Three distinct phases were defined: ferberite (5.01 - 6.00 apfu W), niobian ferberite I (5.00-3.01 apfu W) and *wolframoxiolite* (< 3.00 apfu W) including its U-rich variety (Table 2). They are characterized by large variation in W/(W+Nb+Ta) and calculated Fe<sup>2+</sup>/(Fe<sup>2+</sup>+Fe<sup>3+</sup>) but low and almost constant Mn/(Mn+Fe<sub>tot</sub>) and Ta/(Ta+Nb) (Fig. 5). Subordinate to minor contents of P, U, Ti, Zr, Si, Sc, Al and Ca are particularly typical of *wolframoxiolite* and its U-rich variety. Their concentrations vary from low to negligible in Nb-poor ferberite up to high to moderate in *wolframoxiolite*: UO<sub>2</sub> 2.71, P<sub>2</sub>O<sub>5</sub> 0.30, TiO<sub>2</sub> 4.81, ZrO<sub>2</sub> 2.84, SiO<sub>2</sub> 0.93, Sc<sub>2</sub>O<sub>3</sub> 4.36, Al<sub>2</sub>O<sub>3</sub> 0.87, CaO 1.02 in the first case, and up to UO<sub>2</sub> 19.82, P<sub>2</sub>O<sub>5</sub> 0.27, TiO<sub>2</sub> 4.15, ZrO<sub>2</sub> 2.56, SiO<sub>2</sub> 0.81, Sc<sub>2</sub>O<sub>3</sub> 4.03, Al<sub>2</sub>O<sub>3</sub> 1.37, CaO 0.74 (all in wt.%) in U-rich *wolframoxiolite* (Table 2). Continual decrease of analytical totals from ferberite to *wolframoixiolite* and particularly its W-rich variety is evident. The calculation of Fe<sup>3+</sup> eliminated only small part of this deficiency (Table 2), which seems to be typical of some (W,Nb,Ta)-rich phases (e.g., Ginsburg *et al.*, 1969; Tindle & Webb, 1989).

[Table 2, Fig. 5]

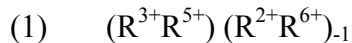
The secondary replacement products – ferberite to niobian ferberite II, tungstenian-titanian ferrocolumbite and niobian and tungstenian rutile (Table 3) - generally show Mn/(Mn+Fe<sup>2+</sup><sub>tot</sub>) and Ta/(Ta+Nb) values comparable to those of the primary phases except rutile with very low Mn/(Mn+Fe<sup>2+</sup><sub>tot</sub>) (Fig. 5). Ferberite to niobian ferberite II exhibits two compositional types with different Fe<sup>2+</sup>/(Fe<sup>2+</sup>+Fe<sup>3+</sup>) values. The abundant Fe<sup>3+</sup>-poor variety is compositionally almost identical with the primary niobian ferberite I except lower variation in W/(W+Nb+Ta). It exhibits sum of cations slightly lower than 12 and R<sup>5+</sup>+W<sup>6+</sup>/R<sup>2+</sup>+R<sup>3+</sup> slightly higher than 1, whereas the rare Fe<sup>3+</sup>-rich variety shows ~1. Tungstenian-titanian ferrocolumbite is evidently impoverished in WO<sub>3</sub> (18.55-29.11 wt.%; 1.12-1.84 *apfu*) but enriched in Nb<sub>2</sub>O<sub>5</sub> (38.52-47.29 wt.%; 4.24-5.01 *apfu*), TiO<sub>2</sub> (4.09-8.08 wt.%; 0.75-1.37 *apfu*), Sc<sub>2</sub>O<sub>3</sub> (2.57-3.29 wt.%; 0.64-0.70 *apfu*) and ZrO<sub>2</sub> (1.48-1.84 wt.%; 0.17-0.22 *apfu*) relative to the associated ferberite to niobian ferberite II. Rutile is highly heterogeneous and two compositional types with different values of W/(W+Nb+Ta), Fe<sup>2+</sup>/(Fe<sup>2+</sup>+Fe<sup>3+</sup>) and Ta/(Ta+Nb) were distinguished (Table 2): a W-rich variety (W>Nb) with WO<sub>3</sub> up to 5.27 wt.% (0.23 *apfu* W) and a Nb-rich variety (Nb>>W) with Nb<sub>2</sub>O<sub>5</sub> up to 13.34 wt.% (1.05 *apfu* Nb); higher Ta/(Ta+Nb) and minor amounts of Zr have been found particularly in the W-rich type, whereas minor amounts of Si and Sc are typical of the Nb-rich type. A ScPO<sub>4</sub> phase is highly heterogeneous and its chemical composition corresponds to an intermediate member between ScPO<sub>4</sub> and ZrSiO<sub>4</sub> with 4-27 mol. % of the zircon component; however, its crystal structure was not confirmed by electron diffraction, as it appears to be amorphous. Very rare secondary scheelite was not quantitatively analyzed.

[Table 3]

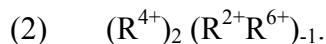
## 5. Discussion

### *Crystal chemistry of primary and secondary phases*

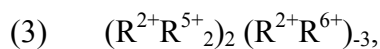
The primary phases include Nb-poor ferberite to compositionally complex *wolframoixiolite*, with a complete miscibility between both phases (Fig. 6). The substitution schemes were derived from R<sup>2+</sup>WO<sub>4</sub> assuming the absence of vacancies and a disordered nature of the crystal structure in these phases. Nevertheless, Graham & Thornber (1974) noted that the cation deficiency in the  $\alpha$ -PbO<sub>2</sub> structural type involving ferberite, *wolframoixiolite*, ferrocolumbite and rutile is not uncommon. Also Beddoe-Stephens & Fortey (1981) suggested vacancy in the A-site of tungstenian columbite. Based on the perfect negative correlation R<sup>5+</sup> versus W (Fig. 6a) the dominant substitution is:



where R<sup>2+</sup> = Fe<sup>2+</sup> > Mn, Ca, Mg, Pb; R<sup>3+</sup> = Fe<sup>3+</sup> > Sc, Al; R<sup>5+</sup> = Nb > Ta, P. However, the perfect negative correlation R<sup>4+</sup> versus R<sup>6+</sup> (Fig. 6b) implies an evident participation of R<sup>4+</sup> cations as well, where R<sup>4+</sup> = Ti > Zr, Hf, Sn, Si, U. It is expressed by the exchange vector:



The positive correlation R<sup>2+</sup> versus R<sup>6+</sup> (Fig. 6c) does not fit a slope close to 1, hence, participation of ferberite-columbite substitution is plausible with the exchange vector:



which could be condensed to:

$$(4) \quad (R^{5+})_4(R^{2+})_{-1}R^{6+}_{-3}$$

Linear regressions of  $R^{6+}$  versus  $R^{5+}$ ,  $R^{4+}$ ,  $R^{3+}$ ,  $R^{2+}$  and  $R^{2+}+R^{3+}$  (Fig. 6), respectively, yielded the following equations:

$$R^{6+} \text{ vs } R^{2+} \quad y=1.13+0.798x \quad r^2=0.959.$$

$$R^{6+} \text{ vs } R^{3+} \quad y=3.35-0.528x \quad r^2=0.797$$

$$R^{6+} \text{ vs } R^{4+} \quad y=1.92-0.343x \quad r^2=0.923$$

$$R^{6+} \text{ vs } R^{5+} \quad y=5.60-0.928x \quad r^2=0.992$$

Consequently, the combination of the (1), (2) and (3) vectors in the approximate ratio 8 : 3 : 2 yielded the combined exchange vector:

$$(5) \quad (R^{3+})_8(R^{4+})_6(R^{5+})_{16}(R^{2+})_{-13}(R^{6+})_{-17},$$

which seems to be the best expression of the actual substitution mechanism. The ratios of  $R^{6+}$  vs  $R^{2+}$  to  $R^{5+}$  are close to the slopes in the above equations. The calculated Nb,Fe<sup>3+</sup>-dominant and W-free end-member composition in the ferberite-wolframoixiolite series is close to  $(R^{2+}_{1.1}R^{3+}_{3.4}R^{4+}_{1.9}R^{5+}_{5.6})_{\Sigma 12}O_{24}$ , which fits quite well the combined substitution vector (5). Some discrepancies illustrated on Fig. 6 may be caused by the vacancy-free formula calculation or the presence of some undetermined light element suggested by the low analytical totals (Table 2). Because the system is poor on Li and Be, small amount of OH in wolframoixiolite may be responsible for these deviations.

[Fig. 6]

Secondary phases include five minerals distinct in their crystal structure and composition: dominant  $\alpha$ -PbO<sub>2</sub> structural type phases – ferberite to niobian ferberite II > tungstenian-titanian ferrocolumbite > niobian and tungstenian rutile (the rare ScPO<sub>4</sub> phase and very rare scheelite were not discussed in detail). The derivation of exchange vectors was done separately for these individual phases. The Fe<sup>3+</sup>-poor variety of ferberite to niobian ferberite II closely follows the same exchange vector as the primary phases (Fig. 7). The very rare Fe<sup>3+</sup>-rich variety is not fully consistent with this substitution scheme and the corresponding exchange vectors were not defined. Derivation of substitution mechanisms of tungstenian-titanian ferrocolumbite and niobian rutile from their precursor primary wolframoixiolite with the mean composition  $\sim (R^{2+}_{2.5}R^{3+}_3R^{4+}_3R^{5+}_3W_{2.5})_{\Sigma 12}O_{24}$  is impossible due to its very high heterogeneity.

[Fig. 7]

Relative to the heterovalent substitutions given above, the homovalent substitutions expressed by the exchange vectors: Fe<sup>2+</sup>Mn<sub>-1</sub>, TaNb<sub>-1</sub> and ScFe<sup>3+</sup><sub>-1</sub> are rather negligible in all primary and secondary phases (Fig. 5). The complete mechanisms for the incorporation of Ca, Zr, Si, P and other minor elements into the structure of the relevant primary and secondary phases were not considered due to their low concentrations, but they were included in the diagrams according to their respective valence charges (Fig. 6, 7). Derivation of the substitution mechanisms given above, however, was very complicated by several factors. We have five substantial components ( $R^{2+}$ ,  $R^{3+}$ ,  $R^{4+}$ ,  $R^{5+}$  and  $R^{6+}$ ) in the system and plotting of feasible diagrams in such a 5-dimensional system is difficult. Moreover, some elements within the individual components may behave in a distinct way in crystal structures of relevant phases,



particularly  $R^{4+}$  cations (e.g. Ti versus U or Ti versus Si). Thus, the derived substitutions are rather approximate.

### *Chemical composition and mechanisms of substitution in W-rich Nb,Ta-oxide minerals from other localities*

Tungsten-rich Nb,Ta-oxide minerals reported from granitic pegmatites and other rare-element granitic rocks show diversified chemical compositions, that mostly fall into the Nb,Fe-dominant part of the columbite quadrilateral. Minerals enriched in Mn and/or Ta also are known (e.g., Konovalenko *et al.*, 1982; Tindle *et al.*, 1998; Raimbault & Burnol, 1998; Aurisicchio *et al.*, 2002). These Nb,Ta-oxide minerals also exhibit highly variable Sn, Ti, Zr, U, Sc, Y, Al and Ca contents.

The compositions of most W-rich Nb,Ta-oxide minerals described up to now are quite different from those of the primary W,Nb,Fe-oxide minerals from Dolní Bory. They commonly exhibit higher Mn/(Mn+Fe<sup>2+</sup><sub>tot</sub>) and Ta/(Ta+Nb) ratios, low concentrations of  $R^{3+}$  (Fe<sup>3+</sup>,Sc), low Zr and Ti, but commonly high Sn contents. The mechanisms of substitution were largely not specified in the original publications except several simple homovalent substitutions, e.g., MnFe<sub>-1</sub> and TaNb<sub>-1</sub> (Ginsburg *et al.*, 1969; v. Knorring & Fadipe, 1981, Konovalenko *et al.*, 1982; Yang *et al.*, 1985; Ranoroosa, 1986; Wang *et al.*, 1988). The following heterovalent substitutions were suggested: in tungstenian columbite from hydrothermal wolframite-quartz veins at Carrock Fell Mine, United Kingdom - (Nb,Ta)<sup>5+</sup><sub>2</sub> (W<sup>6+</sup>Ti<sup>4+</sup>)<sub>-1</sub>, (Sc<sup>3+</sup>Ti<sup>4+</sup>) (Mn,Fe<sup>2+</sup> Nb,Ta<sup>5+</sup>)<sub>-1</sub> and (□2W<sup>6+</sup>) (Mn,Fe<sup>2+</sup> Nb,Ta<sup>5+</sup>)<sub>-1</sub> (Beddoe-Stephens & Fortey, 1981); in tungstenian columbite from rare-element granite at Cínovec, Czech Republic - (R<sup>5+</sup>)<sub>3</sub> (Fe<sup>3+</sup>W<sup>6+</sup>)<sub>-1</sub> and (R<sup>5+</sup>)<sub>2</sub> (R<sup>4+</sup>W<sup>6+</sup>)<sub>-1</sub> (Johan & Johan, 1994); in *wolframowodginite* from complex granitic pegmatites in the Separation Rapids pegmatite group, Ontario, Canada - (Sn<sup>4+</sup>Ta<sup>5+</sup>) (Fe<sup>3+</sup>W)<sub>-1</sub>, (Sn<sup>4+</sup>Ta<sup>5+</sup>) (Mn<sup>2+</sup>W<sup>6+</sup>)<sub>-1</sub> and (Sn<sup>4+</sup>Ta<sup>5+</sup>) (Mn<sup>2+</sup>Ta<sup>5+</sup>W<sup>6+</sup>)<sub>-1</sub> (Tindle *et al.*, 1998); and in niobian ferberite as an exsolution product of W-rich niobian rutile from the Písek pegmatites, Czech Republic - (Fe<sup>2+</sup>)<sub>1</sub> (W<sup>6+</sup>)<sub>3</sub> (Nb<sup>5+</sup>)<sub>-4</sub> (Černý *et al.*, 2007).

The chemical composition of niobian wolframite from the granitic pegmatite at Nuaparra, Mozambique (Saari *et al.*, 1968) is the only one which is close to that of the primary niobian ferberite I from Dolní Bory. It differs in a higher Mn/(Mn+Fe<sup>2+</sup><sub>tot</sub>), absence of Sc, lower Ti and low to trace concentrations of Sn, Sb, Pb, U, Th, Na and Y. Saari *et al.* (1968) suggested that this mineral represents an intermediate solid solution between ferberite Fe<sup>2+</sup>WO<sub>4</sub> and a Fe<sup>3+</sup>NbO<sub>4</sub> phase; consequently, the exchange vectors (1), (2) and (3), operating in the ferberite - *wolframoixiolite* series from Dolní Bory, probably participated. Generally, the chemical composition of the primary *wolframoixiolite* from Dolní Bory is distinct from all other W-rich Nb,Ta-oxide minerals described to date because of the dominance of the Fe<sup>3+</sup>NbO<sub>4</sub> phase. It likely corresponds to a new mineral species described from other localities (see e.g., Ercit, 1994; Černý *et al.*, 1995), but not yet defined.

### *Formation of primary and secondary phases*

Textural relations of the breakdown products are characterized by the total absence of any depleted primary phase in the BSE images; neither *wolframoixiolite* nor niobian ferberite I show any features of depletion. Moreover, ferberite to niobian ferberite II exhibits typically

subhedral shape (Fig. 4b,d). This indicates that the secondary assemblage did not originate by an exsolution-type process found particularly in niobian rutile (e.g., Černý *et al.*, 1998, 1999, 2000a,b, 2007; Černý & Chapman, 2001), where secondary exsolution products are closely associated with a depleted primary phase. In contrast, the secondary phases at Dolní Bory form locally developed aggregates with dominant ferberite to niobian ferberite II and subordinate tungstenian-titanian ferrocolumbite and niobian and tungstenian rutile (plus very rare ScPO<sub>4</sub> and scheelite) with very rare relics of undepleted primary phase (*wolframoixiolite* or niobian ferberite I). Complete recrystallization and reconstitution of the primary minerals seems to be responsible for the origin of the secondary assemblage.

Based on experimental studies (see Perkins *et al.*, 1979; Hemley *et al.*, 1980) and textural relations in the primary mineral assemblage andalusite+diaspore, which hosts W,Nb,Fe-oxide minerals, this assemblage formed at temperatures ~400 °C for P = 2 kbar (Novák & Taylor, 2005). The estimated pressure  $P_{\text{fluid}} = 2$  kbar seems reasonable due to the presence of abundant andalusite. Formation of primary W,Nb,Fe-oxide minerals is closely related chiefly to the assemblage andalusite+diaspore, hence, T < 400°C is very likely for their origin. The breakdown process of primary niobian ferberite-*wolframoixiolite* producing the secondary assemblage probably proceeded at slightly lower temperatures with respect to the primary ones, perhaps approximately in the stability field of pyrophyllite and kaolinite at about 300 °C. These temperatures may be comparable with those of secondary manganotantalite after stibiotantalite or rynersonite, and manganocolumbite after microlite in lepidolite pegmatites from the Moldanubicum estimated to temperatures ~550-350 °C or less (Novák & Černý, 1998b). Nevertheless, Beddoe-Stephens & Fortey (1981) described tungstenian manganocolumbite formed by the breakdown of niobian ferberite associated with the formation of hydrothermal carbonates at T ~250 °C. Consequently, the formation of secondary columbite-group minerals at low temperatures (~300 °C or less) by breakdown of primary Nb,Ta-oxide minerals seems to be very likely. Textural relations at Dolní Bory with no spatial predisposition of secondary phases also suggest minimal, if any, participation of infiltrating fluids in this process.

#### *Miscibility in minerals in the system WO<sub>3</sub> – Nb<sub>2</sub>O<sub>5</sub> – TiO<sub>2</sub> – Fe<sub>2</sub>O<sub>3</sub> – FeO*

The breakdown of compositionally complex primary *wolframoixiolite*-niobian ferberite I containing major Fe<sup>2+</sup>, Fe<sup>3+</sup>, W and Nb, subordinate Ti, Mn and Ca, minor Ta, Zr and Ca, and trace P and Si yielded five newly-formed phases. Hence, mineral association of the W,Nb,Fe-oxide minerals from Dolní Bory may provide clues for understanding the miscibility in the system WO<sub>3</sub> – Nb<sub>2</sub>O<sub>5</sub> – TiO<sub>2</sub> – Fe<sub>2</sub>O<sub>3</sub> - FeO (+ minor Ta<sub>2</sub>O<sub>5</sub>, ZrO<sub>2</sub>, Sc<sub>2</sub>O<sub>3</sub>, MnO) at T < ~400 – 350 °C. During the primary stage at T < ~400 °C, a high miscibility between ferberite Fe<sup>2+</sup>WO<sub>4</sub>, Fe<sup>3+</sup>NbO<sub>4</sub> phase and ferrocolumbite Fe<sup>2+</sup>Nb<sub>2</sub>O<sub>6</sub> is observed (Fig. 7). The Fe<sup>2+</sup>/(Fe<sup>2+</sup>+Fe<sup>3+</sup>) decreasing from primary ferberite to *wolframoixiolite* is associated with increasing of Sc<sub>2</sub>O<sub>3</sub> and TiO<sub>2</sub> in *wolframoixiolite* (Table 2) and indicates the increase of  $f(\text{O}_2)$  during the crystallization of primary W,Nb,Fe-oxide minerals. The  $f(\text{O}_2)$  very likely controls the W incorporation into the *wolframoixiolite* crystal structure; however, in contrast to the tungstenian columbite from Cínovec (Johan & Johan, 1994), W enters the W,Nb,Fe-oxide minerals in Dolní Bory pegmatite at low  $f(\text{O}_2)$ . Continual increasing of Ti in *wolframoixiolite* (Fig. 6, 7) suggests presence of subordinate amount of Ti to stabilize its crystal structure.

Subsequent breakdown yielded minerals with dominant Ti, Nb and/or W and with different crystal structure types and chemical compositions. Tungsten is concentrated chiefly in abundant ferberite to niobian ferberite II and in very rare scheelite; Nb is concentrated dominantly in tungstenian-titanian ferrocolumbite; Ti occurs mainly in rutile. Except the Fe<sup>3+</sup>-rich variety of niobian ferberite II, all these minerals generally have higher Fe<sup>2+</sup>/(Fe<sup>2+</sup>+Fe<sup>3+</sup>) relative to that of primary *wolframoixiolite* (Table 2,3). The presence of two varieties of niobian ferberite and rutile with distinct Fe<sup>2+</sup>/(Fe<sup>2+</sup>+Fe<sup>3+</sup>) values (Table 3) is notable. It may also indicate a polystage breakdown process, which generated metastable disequilibrium products, some of which broke down on continual cooling but some survived. However, some influence of *f*(O)<sub>2</sub> cannot be excluded. The breakdown of *wolframoixiolite* probably occurred at lower temperature and lower *f*(O)<sub>2</sub> relative to its primary crystallization. However, part of the secondary minerals were also formed by the breakdown of primary niobian ferberite I, hence, no significant change in the *f*(O)<sub>2</sub> was necessary. The estimated T of about 350-300 °C is comparable with values reported by Beddoe-Stephens & Fortey (1981).

The secondary W,Nb,Fe-oxide minerals do not occur outside of the ferberite-*wolframoixiolite* zoned crystals. The Ta/(Ta+Nb) and Mn/(Mn+Fe<sup>2+</sup><sub>tot</sub>) values and concentrations of minor elements of the primary and secondary phases disregarding Fe<sup>2+</sup>/(Fe<sup>2+</sup>+Fe<sup>3+</sup>) are very similar (Fig. 5, Table 2,3). This suggests that the secondary minerals originated by bulk-isochemical breakdown of the pre-existing primary phases, without any significant migration of the involved elements and likely at decreasing *f*(O)<sub>2</sub>. The only exception of the cation redistribution within the original grains of primary ferberite-*wolframoixiolite* could have been a local introduction of some Zr and P. The values of Ta/(Ta+Nb) in secondary Nb,Ta-oxide minerals relative to their primary precursors are generally almost constant (Fig. 5; see also Novák & Černý, 1998b; Novák *et al.*, 2004; Wood, 2004), suggesting a very low mobility of these elements during subsolidus reactions. Furthermore, the small variations in Ta/(Ta+Nb) and Mn/(Mn+Fe<sup>2+</sup><sub>tot</sub>) observed in various minerals examined (Fig. 5) are likely controlled by crystal-structural constraints.

### Acknowledgements

The reviews by \_\_\_\_\_ and \_\_\_\_\_, and the editorial improvements by ----- are gratefully acknowledged. S. Houzar from the Moravian Museum, Brno generously provided a part of the samples studied. This work was supported by the research project MSM 0021622412 to MN, and by the Natural Sciences and Engineering Research Council of Canada Major Installation, Major Equipment, Infrastructure and Research Grants to P. Č. and F.C. Hawthorne (University of Manitoba). The authors also thank J. Staněk for comments on an early version of the manuscript.

## References

- Amichba, T.M. & Dubakina, L.S. (1974): Wolframoixiolite in ores of tungsten deposits of Yakutia. *Sborn. Nauchn. Trud. Mosk. Otdel. Vses. Mineral. Obshch.*, **1974**, 11-18 (in Russian)
- Aurischio, C., De Vito, C., Ferrini, V., Orlandi, P. (2001): Nb-Ta oxide minerals from miarolitic pegmatites of the Baveno pink granite, NW Italy. *Mineral. Mag.*, **65**, 509-522.
- \_\_\_\_\_, \_\_\_\_\_, \_\_\_\_\_, \_\_\_\_\_ (2002): Nb and Ta oxide minerals in the Fonte del Prete granitic pegmatite dike, Island of Elba, Italy. *Canad. Mineral.*, **40**, 799-814.
- Beddoe-Stephens, B. & Fortey, N.J. (1981): Columbite from the Carrock Fell tungsten deposit. *Mineral. Mag.*, **44**, 217-223.
- Breiter, K., Škoda, R., Uher, P. (2007): Nb-Ta-Ti-W-Sn-oxide minerals as indicators of a peraluminous P- and F-rich granitic system evolution: Podlesí, Czech Republic. *Mineral. Petrol.*, in print
- Burnham, C.W. (1962): Lattice constant refinement. C. I. W. Year-book, 61, 132-135. New York.
- Černý, P. & Chapman, R. (2001): Exsolution and breakdown of scandian and tungstenian Nb-Ta-Ti-Fe-Mn phases in niobian rutile. *Canad. Mineral.*, **39**, 93 -101.
- \_\_\_\_\_, \_\_\_\_\_, Masau, M. (2000b): Two-stage exsolution of a titanian (Sc,Fe<sup>3+</sup>)(Nb,Ta)O<sub>4</sub> phase in Norwegian niobian rutile. *Canad. Mineral.*, **38**, 907-913.
- \_\_\_\_\_, \_\_\_\_\_, Simmons, W.B., Chackowsky, L.E. (1999): Niobian rutile from the McGuire granitic pegmatite, Park County, Colorado: Solid solution, exsolution, and oxidation. *Amer. Mineral.*, **84**, 754-763.
- Černý, P. & Ercit, S.T. (1985): Some recent advances in the mineralogy and geochemistry of Nb and Ta in rare-element granitic pegmatites. *Bull. Mineral.*, **108**, 499-532.
- \_\_\_\_\_, & \_\_\_\_\_ (1989): Mineralogy of Niobium and Tantalum: Crystal Chemical Relationships, Paragenetic Aspects and Their Economic Implications. In: „Lanthanides, Tantalum and Niobium“, P. Möller, P. Černý, F. Saupe, eds., Springer Verlag Berlin Heidelberg, 27-79.
- \_\_\_\_\_, & \_\_\_\_\_ (2005): The classification of granitic pegmatites revisited. *Canad. Mineral.*, **43**, 2005-2026.
- \_\_\_\_\_, \_\_\_\_\_, Wise, M.A., Buck, H.M. (1998): Compositional, structural and phase relationships in titanian ixiolite and titanian columbite-tantalite. *Canad. Mineral.*, **36**, 547-562.
- Černý, P., Novák, M., Chapman, R., Masau, M. (2000a): Subsolidus behavior of niobian rutile from Věžná, Czech Republic: a model for exsolution in phases with Fe<sup>2+</sup>>>Fe<sup>3+</sup>. *Journ. Czech Geol. Society*, **45**, 21-35.
- \_\_\_\_\_, \_\_\_\_\_, \_\_\_\_\_ (1995): The Al(Nb,Ta)Ti<sub>2</sub> substitution in titanite: the emergence of a new species? *Mineral. Petrol.*, **52**, 61-73
- \_\_\_\_\_, \_\_\_\_\_, \_\_\_\_\_, Ferreira, K.J. (2007): Subsolidus behavior of niobian rutile from Písek region, Czech Republic: a model for exsolution in W- and Fe<sup>2+</sup>>>Fe<sup>3+</sup>-rich phases. *Journal of Geosciences*, in print.
- Duda, J. (1986): Pegmatites in the Bory granulite massif. *Sbor. geol. Věd, Ložisk. geol. mineral.*, **27**, 157-202.

- Ehrenberg, H., Witschek, G., Theissmann, R., Weitzel, H., Fuess, H., Trouw, F. (2000): The magnetic structure of FeNbO<sub>4</sub>. *Journ. Magnet. Magnet. Materials*, **218**, 261-265.
- Ercit, T.S. (1994): The geochemistry and crystal chemistry of columbite-group minerals from granitic pegmatites, southwestern Grenville province, Canadian shield. *Canad. Mineral.*, **32**, 421-438.
- \_\_\_\_\_, Černý, P., Hawthorne, F.C., McCammon, C.A. (1992): The wodginite group. II. Crystal chemistry. *Canad. Mineral.*, **30**, 613-631.
- Garcia-Matres, E., Stusser, N., Hofmann, M., Reehuis, M. (2003): Magnetic phases in Mn<sub>1-x</sub>Fe<sub>x</sub>WO<sub>4</sub> studied by neutron powder diffraction. *Eur. Phys. Journ.*, **B32**, 35-42.
- Ginsburg, A.I., Gorzhenskaya, S.A., Sidorenko, G.A., Ukhina, T.A. (1969): Wolframixiolite, a new variety of ixiolite. *Zapiski Vses. Mineral. Obshch.*, **98**, 63-73 (in Russian).
- Graham, J. & Thornber, M.R. (1974): The crystal chemistry of complex niobium and tantalum oxides I. Structural classification of MO<sub>2</sub> phases. *Amer. Mineral.*, **59**, 1026-1039.
- Hemley, J.J., Montoya, J.W., Marinenko, J.W., Luce, R.W. (1980): Equilibria in the system Al<sub>2</sub>O<sub>3</sub>-SiO<sub>2</sub>-H<sub>2</sub>O and some general implications for alteration/mineralization processes. *Econ. Geol.*, **75**, 210-228.
- Johan, V. & Johan, Z. (1994): Accessory minerals of the Cínovec (Zinnwald) granite cupola, Czech Republic Part 1: Nb-, Ta- and Ti-bearing oxides. *Miner. Petrol.*, **51**, 323-343.
- v. Knorring, O. & Fadipe, A. (1981): On the mineralogy and geochemistry of niobium and tantalum in some granite pegmatites and alkali granites of Africa. *Bull. Minéral.*, **104**, 496-507.
- Konovalenko, S.I., Voloshin, A.V., Pakhomovskiy, Ya.A., Rossovskiy, L.N., Divnev, S.A. (1982): Tungsten-bearing varieties of tantalates-niobates from the miarolitic pegmatites of southwestern Pamir. *Mineral. Zhurnal*, **4**, 65-74 (in Russian).
- Němec, D. (1981): Ein Pegmatit mit Li-Mineralisierung von Dolní Bory, Westmähren (ČSSR). *Chem. d. Erde*, **40**, 146-177.
- Novák, M. & Černý, P. (1998a): Scandium in columbite-group minerals from LCT pegmatites in the Moldanubicum, Czech Republic. *Krystalinikum*, **24**, 73-89.
- \_\_\_\_\_, \_\_\_\_\_ (1998b): Niobium-tantalum oxide minerals from complex pegmatites in the Moldanubicum, Czech Republic; Primary *versus* secondary compositional trends. *Canad. Mineral.*, **36**, 659-672.
- \_\_\_\_\_, \_\_\_\_\_, Čech, F., Staněk, J. (1992): Granitic pegmatites in the territory of the Bohemian and Moravian Moldanubicum. International Symposium on Mineralogy, Petrology and Geochemistry of Granitic Pegmatites, Lepidolite 200, Nové Město na Moravě, 11-20.
- \_\_\_\_\_, \_\_\_\_\_, Cempírek, J., Šrein, V., Filip, J. (2004): Ferrotapiolite as a pseudomorph of stibiotantalite from the Laštovičky lepidolite pegmatite, Czech Republic; an example of hydrothermal alteration on. *Canad. Mineral.*, **42**, 1117-1128.
- \_\_\_\_\_, \_\_\_\_\_, Kimbrough, D.L., Taylor, M.C., Ercit, T.S. (1998): U-Pb Ages of monazite from granitic pegmatites in the Moldanubicum and their geological implications.

- POCEEL international symposium, Praha, September 30-October 2, Acta Univ. Carol., Geol., 42, 2, 309-310.
- Novák, M. & Šrein, V. (1989): Chemical composition and paragenesis of ferberite from the Dolní Bory pegmatites, western Moravia, Czechoslovakia. *Acta Univ. Carol., Geol., Cech Vol.*, 495-500.
- Novák, M. & Staněk, J. (1999): Pegmatite from Dobrá Voda. *Acta Mus. Moraviae, Sci. geol.*, **84**, 3-44. (in Czech with English Summary).
- Novák, M. & Taylor, M.C. (2005): Andalusite+diaspore nodule in the quartz core from barren pegmatite at Dolní Bory, Czech Republic: an example of primary crystallization from a sol-gel medium. International Meeting on Crystallization processes in granitic pegmatites. Elba, May 2005.
- Ondruš, P. & Skála, R. (1997): New quasi-empirical channel Search/Match algorithm for ICDD PDF2 Database: A tool for qualitative phase analysis integrated in the ZDS System software package for X-ray powder diffraction analysis. Fifth European Powder Diffraction conference EPDIC-5, Parma.
- Perkins, D. III., Essene, E.J., Westrum, E.F. Jr., Wall, V.J. (1979): New thermodynamic data for diaspore and their application to the system  $Al_2O_3-SiO_2-H_2O$ . *Amer. Mineral.*, **64**, 1080-1090.
- Pouchou, J.L. & Pichoir, F. (1984): A new model for quantitative analysis. I. Application to the analysis of homogeneous samples. *La Recherche Aérop.*, **3**, 13-38.
- \_\_\_\_\_ & \_\_\_\_\_ (1985): "PAP"(φ-ρ-Z) procedure for improved quantitative microanalysis. In: "Microbeam Analysis", J. T. Armstrong, ed., San Francisco Press, 104-106.
- Raimbault, L. & Burnol, L. (1998): The Richemont rhyolite dyke, Massif Central, France; a subvolcanic equivalent of rare-element granites. *Canad. Mineral.*, **36**, 265-282.
- Ranoroosa, N. (1986): Etude mineralogique et microthermometrique des pegmatites du champ de la Sahatany - Madagascar. PhD. thesis, Universite Paul Sabatier, Toulouse.
- Saari, E., v. Knorring, O., Sahama, Th.G. (1968): Niobian ferberite from the Nuaparra pegmatite, Zambezia, Mozambique. *Lithos*, **1**, 64-68.
- Škoda, R., Novák, M., Houzar, S. (2006): Granitic NYF pegmatites of the Třebíč Pluton (Czech Republic). *Acta Mus. Moraviae, Sci. geol.*, 91, 129-176. (in Czech with English Summary).
- \_\_\_\_\_, Staněk, J., Čopjaková, R., (2007): Mineral assemblages of the phosphate nodules from the granitic pegmatite at Cyrilov near Velké Meziříčí, Moldanubicum; part I-primary and exsolution phases. *Acta Mus. Moraviae, Sci. geol.*, 92, 59-74. (in Czech with English Summary)
- Staněk, J. (1954): Petrography and mineralogy of pegmatite dikes near Dolní Bory. *Práce Brněn. Zákł. Cs. Akad. Věd*, **26**, 1-43. (in Czech).
- \_\_\_\_\_ (1968): Triplite, cassiterite and topaz from pegmatite near Rousměrov, Western Moravia. *Folia přír. fak. UJEP*, **14**, 71-81.
- \_\_\_\_\_ (1973): Mineral paragenesis of the new lithium-bearing pegmatite at Laštovičky, western Moravia, Czechoslovakia. *Scripta přír. fak. UJEP*, **3**, 1-14.

- \_\_\_\_ (1997): Mineral assemblages of significant pegmatite dikes from the Hatě area near Dolní Bory, Western Moravia. *Acta Mus. Moraviae, Sci. nat.*, 82, 3 – 19. (in Czech with English Summary).
- Tindle, A.G., Breaks, R.W., Webb, P.C. (1998): Wodginite-group minerals from the Separation Rapids rare-element granitic pegmatite group, northwestern Ontario. *Canad. Mineral.*, 36, 637-658.
- \_\_\_\_ & Webb, P.C. (1989): Niobian wolframite from Glen Gairn in the Eastern Highlands of Scotland: A microprobe investigation. *Geochim. Cosmochim Acta*, 53, 1921-1935.
- Wang, S., Ma, Z., Peng, Z. (1988): The crystal structure of wolframixiolite. *Kexue Tongbao (Foreign Language Edition)*, 33, 1363-1366.
- Wood, S. (2004): The aqueous geochemistry of zirconium, hafnium, niobium and tantalum. In: “Short Course Notes, Rare Element Geochemistry and Ore Deposits”, R.L. Linnen, I.M. Samson, Vol. 17., 329-405.
- Yang, G., Wang, S., Peng, Z., Bu, J. (1985): Qitalingite - A newly discovered superstructure complex oxide. *Acta Mineral. Sinica*, 5, 193-198 (in Chinese).

**Figure captions:**

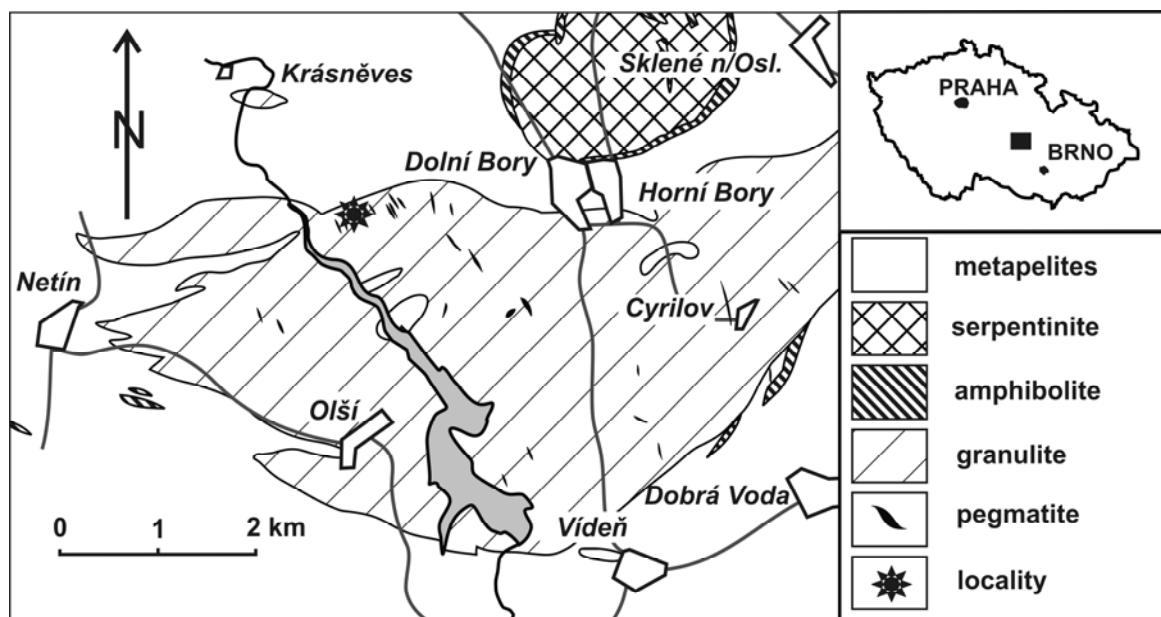


**Fig.1.** Schematic geological map of the Bory pegmatite district (modified from Duda 1986); location of the No. 3 pegmatite.

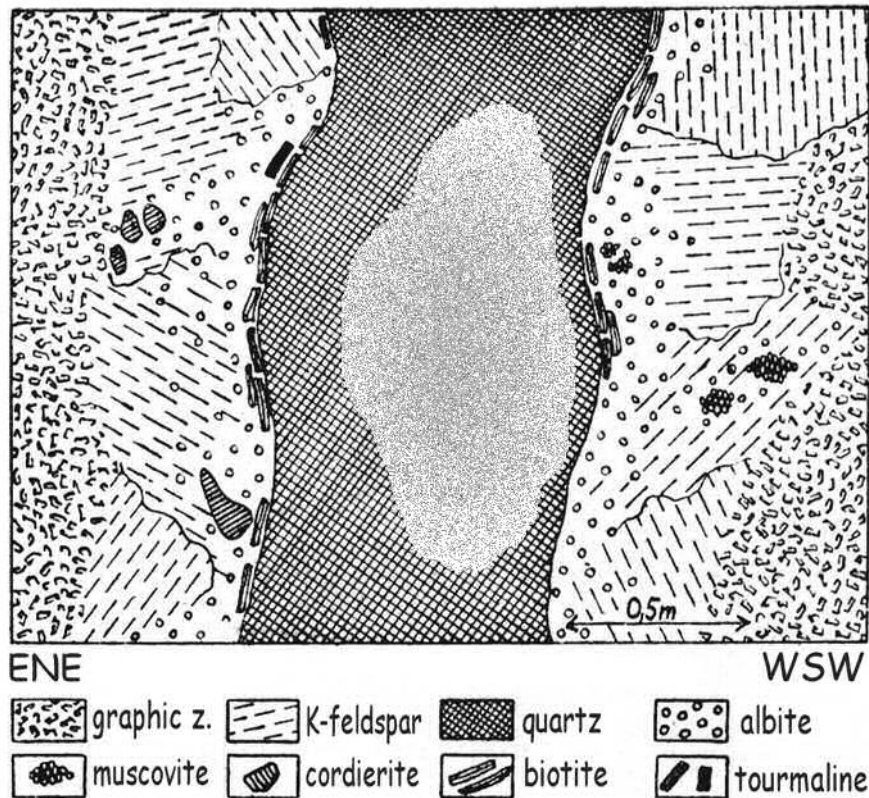


**Fig. 2.** Idealized cross section through the Dolní Bory pegmatite; modified from Staněk (1954). Shaded area in quartz core is andalusite-diaspore nodule.

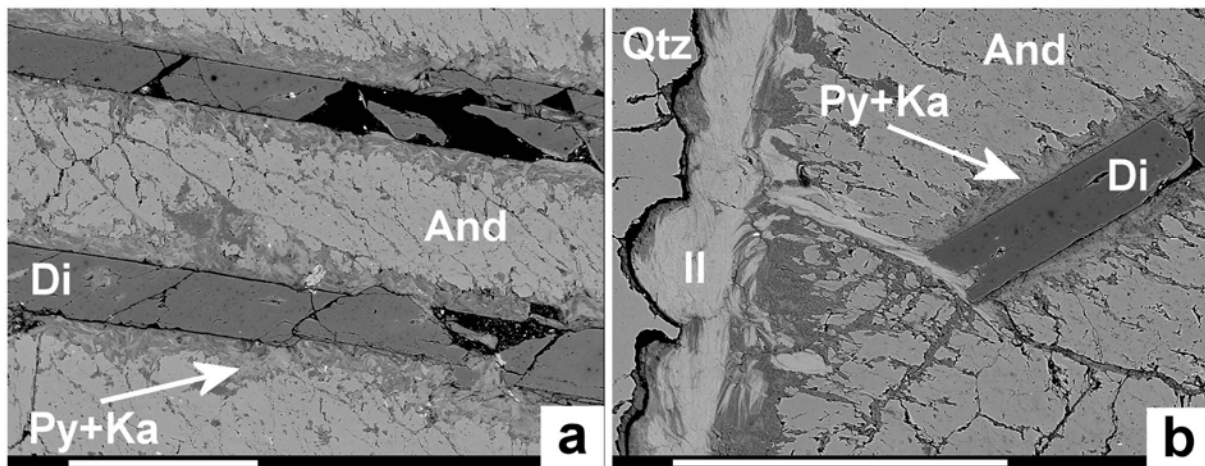


**Fig. 3.** BSE images of the textural relations in the andalusite-diaspore nodule. Scale bar = 500  $\mu\text{m}$ . a) broken lamellae of diaspore (Di) in undeformed andalusite (And), which is replaced by pyrophyllite (Py) and kaolinite (Ka). b) broken lamella of diaspore in andalusite replaced by pyrophyllite, kaolinite and illite-muscovite (Il) concentrated particularly along the contact with quartz (Qtz).



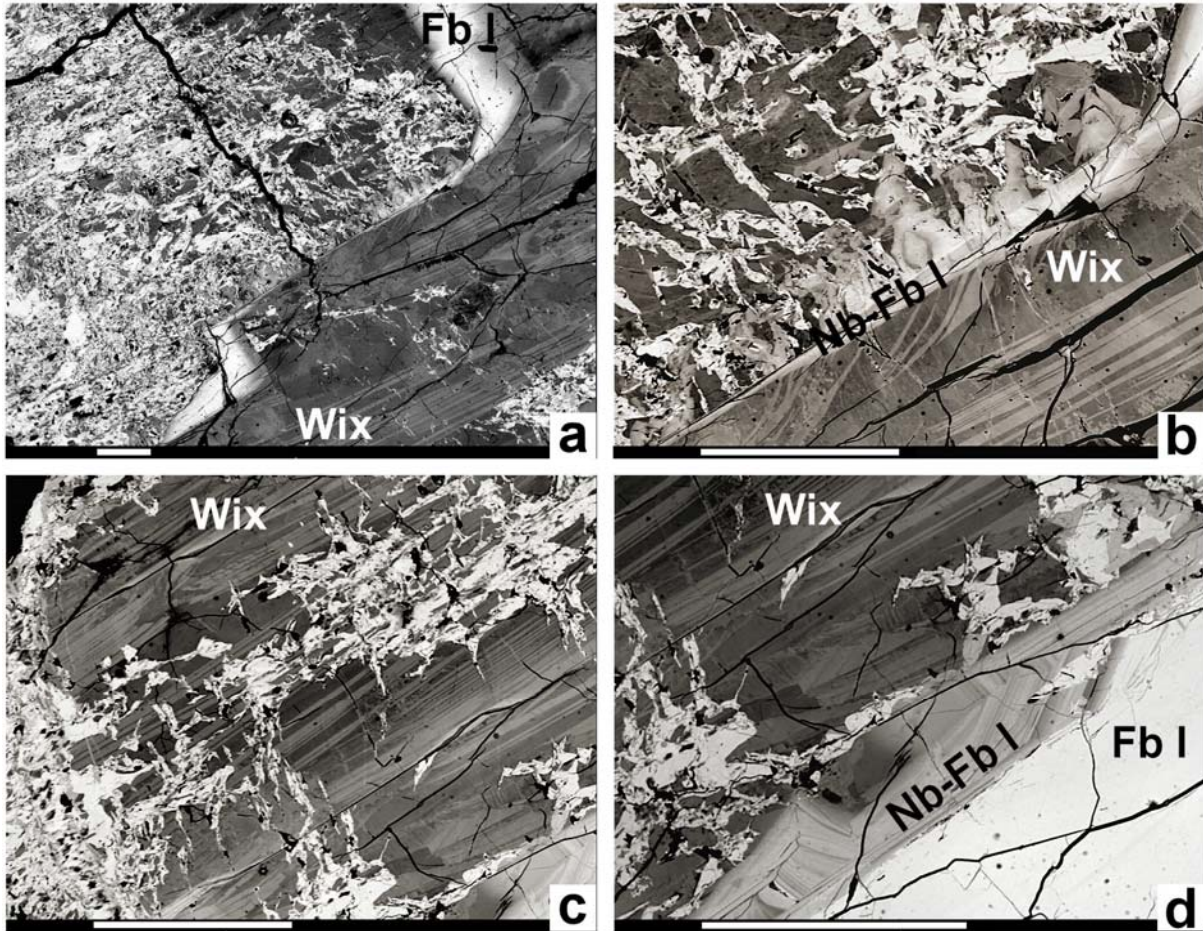


**Fig. 4.** BSE image of a primary ferberite-*wolframoixiolite* crystal, oscillatory zoned from ferberite (Fb I - white) to niobian ferberite I (Nb-Fb I - pale gray) and heterogeneous *wolframoixiolite* Wix (dark gray). Note abundant aggregates of secondary breakdown products – ferberite to niobian ferberite II, tungstenian-titanian ferrocolumbite, and niobian and tungstenian rutile. Scale bar = 100  $\mu\text{m}$  in all figures. a) irregular distribution of the secondary breakdown products in zoned ferberite-*wolframoixiolite* concentrated particularly in *wolframoixiolite* portions; b) secondary aggregate of ferberite to niobian ferberite II (pale) and ferrocolumbite (gray) in heterogeneous *wolframoixiolite* with fine oscillatory zones of niobian ferberite I (pale) (detail of the Fig. a); c) the network of fine bright grains consists of subhedral secondary ferberite to niobian ferberite II in complexly zoned *wolframoixiolite*; d) primary ferberite (white) and oscillatory zoned niobian ferberite I to *wolframoixiolite* (dark), note distinct abundances of secondary ferberite to niobian ferberite II in the primary niobian ferberite I and in *wolframoixiolite*, and heterogeneous composition of secondary ferberite to niobian ferberite II (upright part).

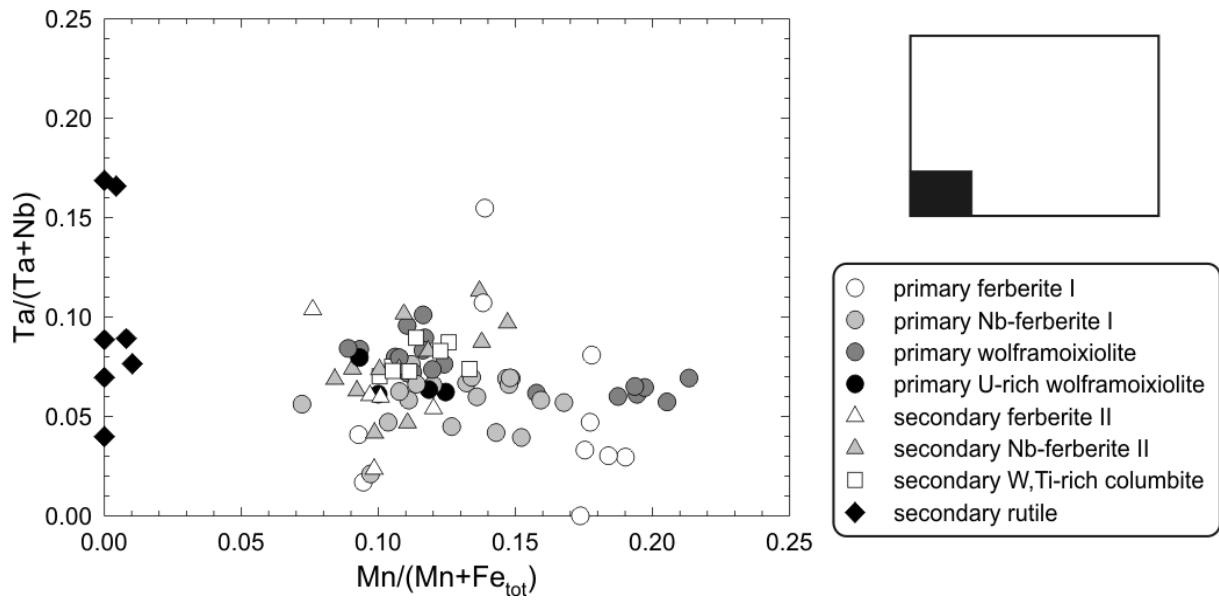


**Fig. 5.** Primary and secondary W,Nb,Fe-oxide minerals from the pegmatite No. 3, Dolní Bory - Hatě in the columbite quadrilateral.

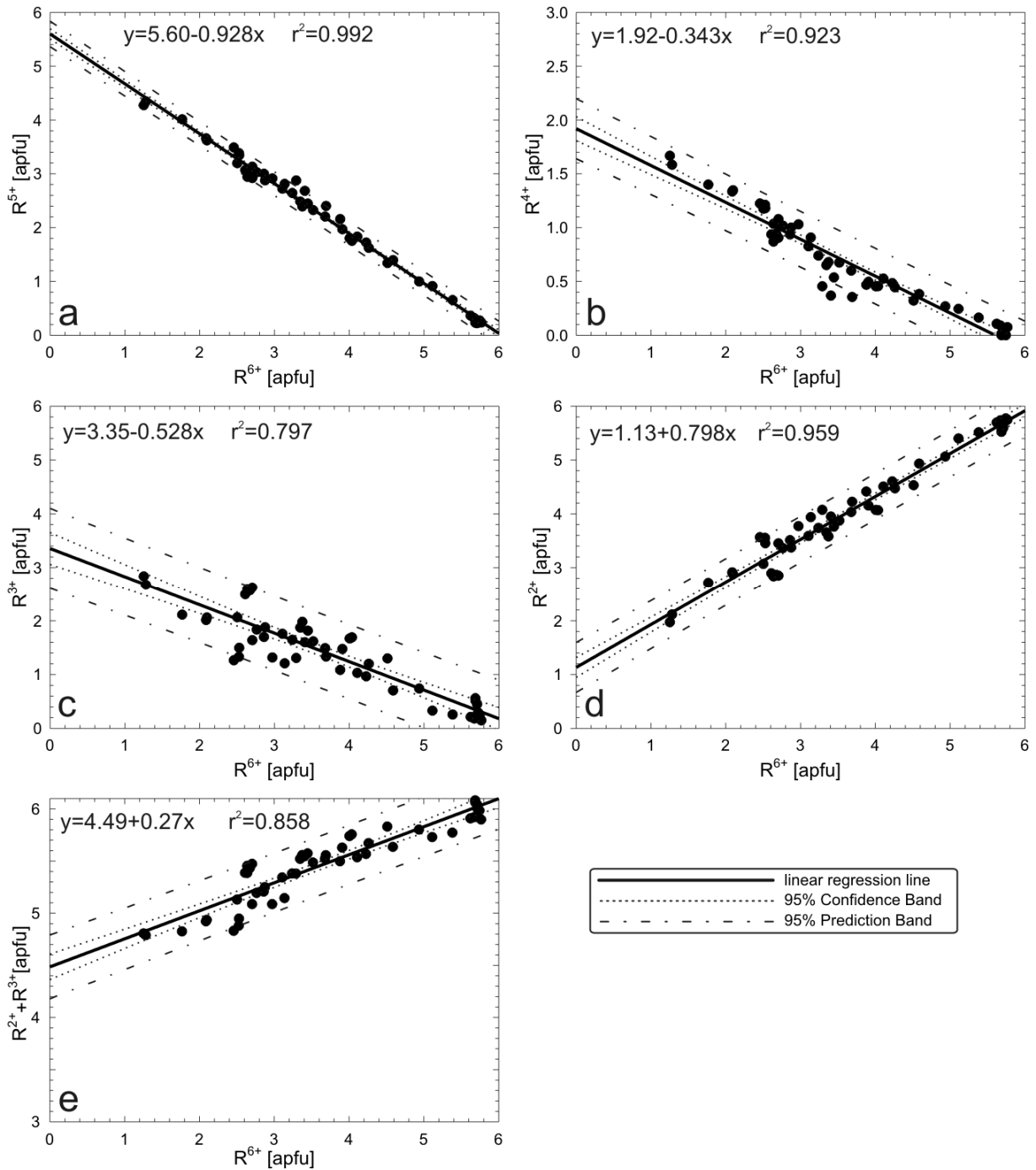


**Fig. 6.** Correlation of the terms: a)  $R^{6+}$  vs  $R^{5+}$ , b)  $R^{6+}$  vs  $R^{4+}$ , c)  $R^{6+}$  vs  $R^{3+}$ , d)  $R^{6+}$  vs  $R^{2+}$ , e)  $R^{6+}$  vs  $R^{2+}+R^{3+}$  in primary ferberite, niobian ferberite I and wolframoixiolite.

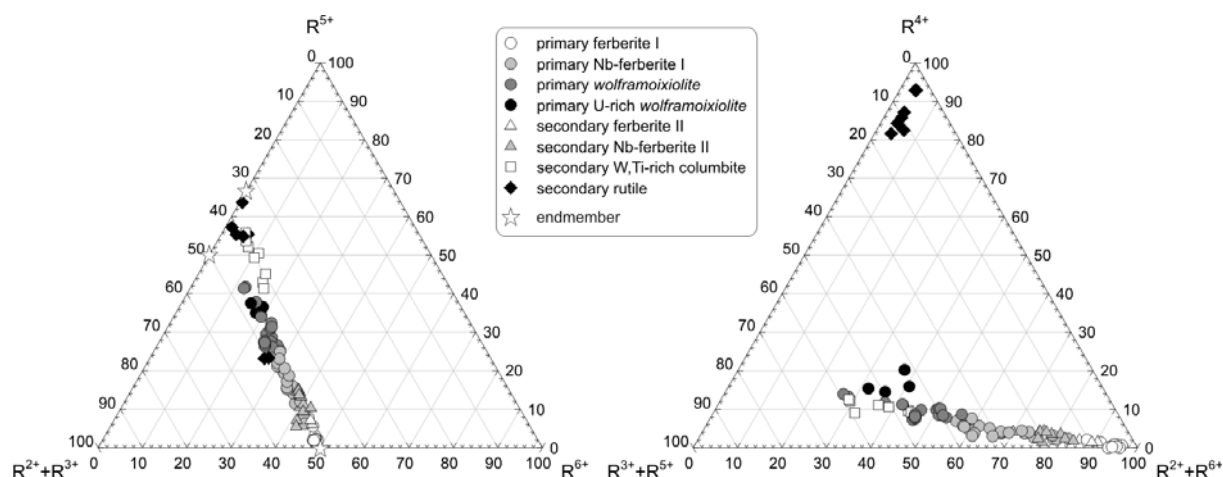










**Fig. 7.** Compositions of primary and secondary W,Nb,Fe-oxide minerals from Dolní Bory - Hatě in the ternary diagrams. a)  $(R^{2+}+R^{3+}) - (R^{5+}) - (R^{6+})$ ; b)  $(R^{2+}+R^{5+}) - (R^{4+}) - (R^{2+}+R^{6+})$ .

### Tables:

	<i>a</i>	<i>b</i>	<i>c</i>	$\beta$	Source
<b>niobian ferberite</b>	4.746(1)	5.722(1)	4.979(1)	90.05(2)	this work
<b>niobian ferberite</b>	4.734(6)	5.739(7)	4.979(3)	90.10(20)	this work
$Fe^{2+}WO_4$ synth.	4.73022(6)	5.70578(7)	4.95230(5)	89.7268(8)	Garcia-Matres <i>et al.</i> (2003)
$Fe^{3+}NbO_4$ synth.	4.6456(1)	5.6151(1)	4.9965(1)	89.85(1)	Ehrenberg <i>et al.</i> (2000)
niobian ferberite	4.735(10)	5.726(10)	5.090(10)	90.00	Saari <i>et al.</i> (1968)
wolframoixiolite	4.750	5.72	5.06	90.00	Ginsburg <i>et al.</i> (1969)
wolframoixiolite	4.674(2)	5.673(1)	5.050(1)	90.00	Wang <i>et al.</i> (1988)

**Table 1.** Unit-cell dimensions of some Nb,Ta,W-oxide minerals from Dolní Bory.

	Fb-I 	Fb-I 	Nb-Fb-I 	Nb-Fb-I 	Nb-Fb-I 	Wix 	Wix 	U-Wix 
WO <sub>3</sub>	74.13	72.63	61.20	50.64	49.32	40.23	37.32	23.64
Ta <sub>2</sub> O <sub>5</sub>	0.00	0.15	0.67	1.90	2.20	2.55	3.76	2.69
Nb <sub>2</sub> O <sub>5</sub>	1.76	2.60	9.87	19.27	18.74	23.62	26.21	24.85
P <sub>2</sub> O <sub>5</sub>	n.d.	0.00	0.08	0.10	0.00	0.17	0.11	0.22
TiO <sub>2</sub>	0.07	0.10	0.47	2.15	2.45	3.34	3.58	2.98
SiO <sub>2</sub>	n.d.	0.02	0.24	0.10	0.03	0.24	0.58	0.89
SnO <sub>2</sub>	n.d.	0.03	0.05	n.d.	n.d.	n.d.	0.12	0.03
ZrO <sub>2</sub>	n.d.	0.47	0.90	0.68	1.44	1.90	2.18	1.72
HfO <sub>2</sub>	n.d.	0.01	0.07	n.d.	n.d.	n.d.	0.16	0.06
UO <sub>2</sub>	n.d.	0.06	0.21	n.d.	n.d.	n.d.	0.95	19.82
ThO <sub>2</sub>	n.d.	0.02	0.03	n.d.	n.d.	n.d.	0.02	0.00
Al <sub>2</sub> O <sub>3</sub>	n.d.	0.00	0.25	n.d.	n.d.	n.d.	0.54	1.24
Sc <sub>2</sub> O <sub>3</sub>	0.77	0.66	1.58	2.49	3.15	3.67	3.23	2.64
*Fe <sub>2</sub> O <sub>3</sub>	1.41	0.18	3.85	6.29	6.32	9.06	2.17	2.27
*FeO	18.30	18.32	15.10	15.22	12.46	8.13	13.58	8.72
MnO	4.06	3.88	3.29	1.60	3.10	3.88	1.85	1.18
PbO	n.d.	0.00	0.36	n.d.	n.d.	n.d.	0.60	0.67
MgO	n.d.	0.30	0.14	n.d.	n.d.	n.d.	0.07	0.13
CaO	0.00	0.02	0.20	0.23	0.49	1.02	0.39	0.75
Total	100.50	99.45	98.56	100.67	99.69	97.81	97.43	94.50
calculated on the basis of 12 cations and 24 oxygens								
W <sup>6+</sup>	5.687	5.621	4.510	3.445	3.371	2.673	2.524	1.766
Ta <sup>5+</sup>	-	0.012	0.052	0.136	0.158	0.178	0.267	0.211
Nb <sup>5+</sup>	0.236	0.351	1.269	2.287	2.237	2.737	3.093	3.239
P <sup>5+</sup>	-	0.000	0.019	0.022	0	0.037	0.024	0.054
Ti <sup>4+</sup>	0.016	0.022	0.101	0.424	0.486	0.644	0.703	0.646
Si <sup>4+</sup>	-	0.006	0.068	0.026	0.008	0.062	0.151	0.257
Sn <sup>4+</sup>	-	0.004	0.006	-	-	-	0.012	0.003
Zr <sup>4+</sup>	-	0.068	0.125	0.087	0.185	0.237	0.277	0.242
Hf <sup>4+</sup>	-	0.001	0.006	-	-	-	0.012	0.005
U <sup>4+</sup>	-	0.004	0.013	-	-	-	0.055	1.271
Th <sup>4+</sup>	-	0.001	0.002	-	-	-	0.001	0.000
Al <sup>3+</sup>	-	0.000	0.084	-	-	-	0.166	0.421
Sc <sup>3+</sup>	0.199	0.172	0.392	0.569	0.724	0.82	0.735	0.663
*Fe <sup>3+</sup>	0.315	0.040	0.823	1.243	1.254	1.748	0.427	0.492
*Fe <sup>2+</sup>	4.53	4.576	3.591	3.34	2.748	1.742	2.965	2.102
Mn <sup>2+</sup>	1.018	0.981	0.792	0.356	0.693	0.842	0.409	0.288
Pb <sup>2+</sup>	-	0.000	0.028	-	-	-	0.042	0.052
Mg <sup>2+</sup>	-	0.134	0.059	-	-	-	0.027	0.056
Ca <sup>2+</sup>	-	0.006	0.061	0.065	0.138	0.28	0.109	0.232
Σ cat.	12.000	12.000	12.000	12.000	12.000	12.000	12.000	12.000
O	24	24	24	24	24	24	24	24

**Table 2.** Representative chemical compositions of primary W,Nb,Fe-oxide minerals from Dolní Bory - Hatě. Fb I- ferberite, Nb-Fb I – niobian ferberite, Wix – wolframoixiolite, U-Wix – U-rich wolframoixiolite.

	Fb-II ▲	Nb-Fb-II ▲	Nb-Fb-II ▲	Nb-Fb-II ▲	W,Ti-Col □	W,Ti-Col □	W,Ti-Col □	W,Ti-Col □	Rt ◆	Rt ◆
WO <sub>3</sub>	70.43	64.00	59.87	60.99	19.21	29.11	18.55	9.60	1.44	5.27
Ta <sub>2</sub> O <sub>5</sub>	0.21	1.07	1.58	1.52	6.18	4.84	6.15	8.54	3.69	0.34
Nb <sub>2</sub> O <sub>5</sub>	5.36	9.55	12.86	11.56	47.29	38.52	46.33	52.24	11.14	2.39
P <sub>2</sub> O <sub>5</sub>	n.d.	0.00	0.00	0.00	0.00	0.00	n.d.	n.d.	0.01	n.d.
TiO <sub>2</sub>	0.41	1.01	1.29	1.16	5.96	4.09	5.65	8.08	77.71	87.59
SiO <sub>2</sub>	0.15	0.00	0.00	0.00	0.00	0.00	1.14	0.00	0.04	0.80
SnO <sub>2</sub>	n.d.	0.07	0.05	0.08	0.07	0.08	n.d.	n.d.	0.09	n.d.
ZrO <sub>2</sub>	0.28	1.28	1.64	1.64	1.71	1.68	0.64	1.22	0.08	0.00
HfO <sub>2</sub>	n.d.	0.11	0.05	0.08	0.06	0.07	n.d.	n.d.	0.03	n.d.
UO <sub>2</sub>	n.d.	0.03	0.02	0.01	0.06	0.03	n.d.	n.d.	0.01	n.d.
ThO <sub>2</sub>	n.d.	0.03	0.00	0.00	0.00	0.00	n.d.	n.d.	0.00	n.d.
Al <sub>2</sub> O <sub>3</sub>	n.d.	0.04	0.03	0.04	0.02	0.02	n.d.	n.d.	0.31	n.d.
Sc <sub>2</sub> O <sub>3</sub>	1.04	2.21	2.64	2.57	3.20	3.29	1.78	2.72	0.16	0.21
Fe <sub>2</sub> O <sub>3</sub>	0.00	0.00	0.00	0.00	0.00	1.91	4.02	3.82	2.27	1.32
FeO	20.33	19.08	18.73	18.51	15.56	15.53	13.85	13.21	2.71	1.57
MnO	2.19	1.91	1.70	2.04	1.81	1.90	2.65	2.11	0.02	0.03
PbO	n.d.	0.00	0.06	0.03	0.23	0.12	n.d.	n.d.	0.03	n.d.
MgO	n.d.	0.08	0.07	0.14	0.13	0.07	n.d.	n.d.	0.00	n.d.
CaO	n.d.	0.02	0.01	0.01	0.01	0.01	n.d.	n.d.	0.00	n.d.
Total	100.40	100.49	100.60	100.38	101.50	101.27	100.76	101.54	99.74	99.52
calculated on the basis of 12 cations and 24 oxygens										
W <sup>6+</sup>	5.319	4.690	4.304	4.419	1.167	1.836	1.119	0.561	0.064	0.228
Ta <sup>5+</sup>	0.017	0.082	0.119	0.116	0.394	0.320	0.389	0.524	0.173	0.015
Nb <sup>5+</sup>	0.706	1.221	1.613	1.461	5.013	4.239	4.877	5.329	0.870	0.181
P <sup>5+</sup>	-	0.000	0.000	0.000	0.000	0.000	-	-	0.001	-
Ti <sup>4+</sup>	0.090	0.215	0.269	0.244	1.051	0.749	0.989	1.371	10.092	11.013
Si <sup>4+</sup>	0.044	0.000	0.000	0.000	0.000	0.000	0.265	0.000	0.007	0.134
Sn <sup>4+</sup>	-	0.008	0.006	0.009	0.007	0.008	-	-	0.006	-
Zr <sup>4+</sup>	0.040	0.177	0.222	0.224	0.196	0.199	0.073	0.134	0.007	0.000
Hf <sup>4+</sup>	-	0.009	0.004	0.006	0.004	0.005	-	-	0.001	-
U <sup>4+</sup>	-	0.002	0.001	0.001	0.003	0.002	-	-	0.000	-
Th <sup>4+</sup>	-	0.002	0.000	0.000	0.000	0.000	-	-	0.000	-
Al <sup>3+</sup>	-	0.013	0.010	0.013	0.006	0.006	-	-	0.063	-
Sc <sup>3+</sup>	0.264	0.545	0.638	0.626	0.654	0.698	0.361	0.535	0.024	0.031
Fe <sup>3+</sup>	0.000	0.000	0.000	0.000	0.000	0.350	0.705	0.649	0.294	0.166
Fe <sup>2+</sup>	4.954	4.512	4.345	4.328	3.051	3.162	2.697	2.493	0.392	0.220
Mn <sup>2+</sup>	0.541	0.458	0.399	0.483	0.359	0.392	0.523	0.403	0.003	0.004
Pb <sup>2+</sup>	-	0.000	0.004	0.002	0.015	0.008	-	-	0.001	-
Mg <sup>2+</sup>	-	0.034	0.029	0.058	0.045	0.025	-	-	0.000	-
Ca <sup>2+</sup>	-	0.006	0.003	0.003	0.003	0.003	-	-	0.000	-
Σ cat.	11.973	11.973	11.967	11.993	11.966	12.000	12.000	12.000	12.000	12.000
O	24	24	24	24	24	24	24	24	24	24

**Table 3.** Representative chemical compositions of secondary phases from Dolní Bory - Hatě. Fb II- ferberite, Nb-Fb II – niobian ferberite, W,Ti-Col – tungstenian and titanian ferrocolumbite, Rt – tungstenian and niobian rutile.